



HAL
open science

POINT DEFECTS OF LOW SYMMETRY IN $KZnF_3$ SINGLE CRYSTALS

M. Binois, A. Leble, J. Rousseau, Jérôme Fayette

► **To cite this version:**

M. Binois, A. Leble, J. Rousseau, Jérôme Fayette. POINT DEFECTS OF LOW SYMMETRY IN $KZnF_3$ SINGLE CRYSTALS. *Journal de Physique Colloques*, 1973, 34 (C9), pp.C9-285-C9-288. 10.1051/jphyscol:1973950 . jpa-00215425

HAL Id: jpa-00215425

<https://hal.science/jpa-00215425>

Submitted on 4 Feb 2008

HAL is a multi-disciplinary open access archive for the deposit and dissemination of scientific research documents, whether they are published or not. The documents may come from teaching and research institutions in France or abroad, or from public or private research centers.

L'archive ouverte pluridisciplinaire **HAL**, est destinée au dépôt et à la diffusion de documents scientifiques de niveau recherche, publiés ou non, émanant des établissements d'enseignement et de recherche français ou étrangers, des laboratoires publics ou privés.

POINT DEFECTS OF LOW SYMMETRY IN KZnF_3 SINGLE CRYSTALS

M. BINOIS, A. LEBLE, J. J. ROUSSEAU and J. C. FAYET

Laboratoire de spectroscopie du solide
Faculté des Sciences, 72000 Le Mans, France

Résumé. — On présente des résultats expérimentaux sur des monocristaux de KZnF_3 dopés avec des ions trivalents (Fe^{3+} et Cr^{3+}) ou irradiés avec des rayons X à 77 K ou à 300 K. Quelques propriétés des défauts créés par ces traitements sont décrites.

Abstract. — We present experimental results on KZnF_3 single crystals doped with trivalent ions (Fe^{3+} and Cr^{3+}) or irradiated with X-rays at 77 K or 300 K. Some properties of the induced defects are described.

Single crystals of KZnF_3 , grown either by means of a flux technique or by a Bridgman method, have been doped with trivalent ions (Fe^{3+} , Cr^{3+}) or submitted to X-rays at various temperatures in the range 77-300 K. Both treatments give rise to point defects of low symmetry (C_{4v} , C_{3v} , C_{2v}).

We report ESR data on charge compensation systems in doped crystals and the results of investigations, of radiation-induced defects, by means of optical techniques. Optical bleaching with polarized light has been shown to result in dichroic absorption, characteristic of $\langle 110 \rangle$ oriented centers at 360 nm, and $\langle 111 \rangle$ oriented centers at 390, 270 and 230 nm.

1. ESR Measurements on KZnF_3 ; Cr^{3+} . — Trivalent Cr^{3+} is substituted for divalent Zn^{2+} in the fluoperovskite lattice (Fig. 1). The ESR spectrum of

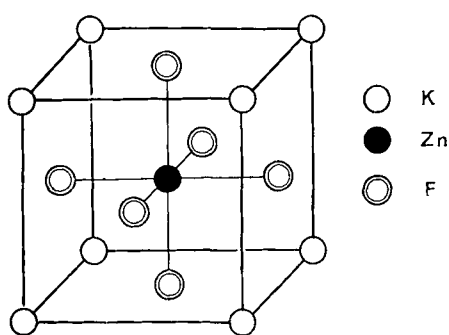


FIG. 1. — Fluoperovskite lattice.

a heavily doped crystal (one per cent in the melt) is shown in figure 2. The magnetic field is along $\langle 001 \rangle$ direction.

Many Cr^{3+} ions enter purely cubic site and are responsible of the intense central line. The adjacent A lines arise from Cr^{3+} ions in tetragonal sites. As a proof, the intensity of the lines denoted A_{\perp} (distortion along $\langle 010 \rangle$ or $\langle 100 \rangle$) is twice the intensity of

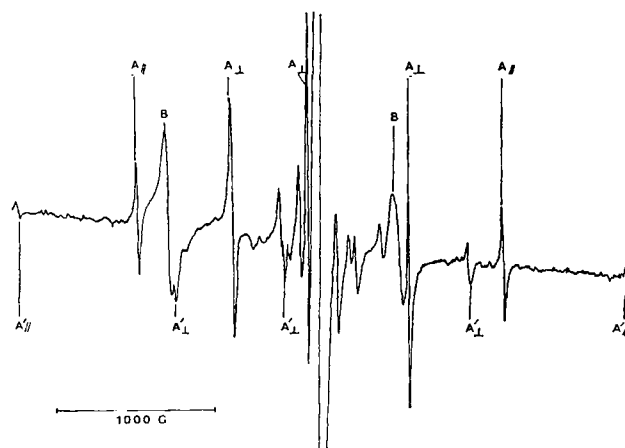


FIG. 2. — ESR spectrum, at room temperature, of heavily Cr^{3+} doped KZnF_3 . H is along a $\langle 001 \rangle$ axis.

the lines denoted A_{\parallel} (distortion along $\langle 001 \rangle$), while their displacement ratio is nearly 1 : 2. The lines denoted B arise from Cr^{3+} ions in trigonal sites, since only one set of lines is observed when H is along a cubic axis.

The values of the spin hamiltonian parameters for the cubic, tetragonal and trigonal sites are listed in table I.

1.1 CUBIC SITE. — Measurements of the structure of the relative EPR line, when H is parallel to $\langle 001 \rangle$ and $\langle 111 \rangle$ directions lead to an unambiguous determination of the fluorine superhyperfine interaction (Table I). The spectrum, for $H // \langle 111 \rangle$, at first sight, looks as due to seven lines of relative intensity (1, 6, 15, 20, 15, 6, 1). The actual structure is far more complicated. Because of fluorine nuclei reorientation, the electronic transitions ($M_S : \pm \frac{3}{2} \leftrightarrow \pm \frac{1}{2} ; -\frac{1}{2} \rightarrow \frac{1}{2}$), give rise to different sup. hyperfine structures made of forty nine lines [1]. The calculated spectrum, assuming gaussian line, line width being

TABLE I

Hamiltonian spin parameters of Cr^{3+} and Fe^{3+} in KZnF_3 . All entries are in 10^{-4} cm^{-1} except g

Cr^{3+}	Cubic	$g = 1.9735 (*)$		$^{53}A = 17,6 (*)$	$A_{\parallel} = -8,85 (*)$ $A_{\perp} = 2,85 (*)$	
	Tetragonal	I	$g_{\parallel} = 1.9757$ $g_{\perp} = 1.9785$	$D = 540,9$		$A_{\parallel 1} = -7,7$ $A_{\parallel 2} = -11,2$ $A_{\perp 3,4,5,6} = 2,0$
		II	$g_{\parallel} = 1.9708$ $g_{\perp} = 1.9766$	$D = 900$		
	Trigonal		$g_{\parallel} = 1.974$ $g_{\perp} = 1.978$	$D = 1542$		
Fe^{3+}	Cubic (i)	$g = 2.0030$	$a = 52,7$ $a = 56,9 (*)$	$^{57}A = 9,4 (*)$	$A_{\parallel} = 35,99 (*)$ $A_{\perp} = 17,192 (*)$	
	Tetragonal	$\langle g \rangle = 1.99$	$D = 740$ $a + \frac{3}{2}F = 63$ $D = 107,9 (*)$			
	Trigonal (ii)	$g = 2.0029 (*)$	$a = 49,7 (*)$ $F = -2,7 (*)$			

(*) Measured at liquid nitrogen temperature.

(i) See [6].

(ii) See [4].

15 G for $M_s : \pm \frac{3}{2} \leftrightarrow \pm \frac{1}{2}$, 2.25 G for $M_s : -\frac{1}{2} \rightarrow +\frac{1}{2}$, fits [2] quite well with the observed curve, as shown in figure 3.

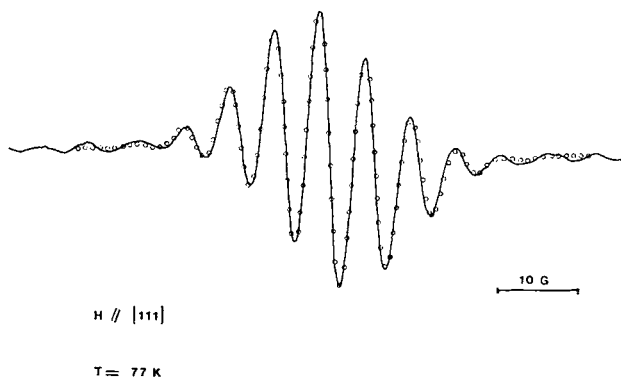


FIG. 3. — Cubic site shf structure of the EPR line. H is along a $\langle 111 \rangle$ axis. Full line: experimental curve. Small lines on each side of the main line are due to ^{53}Cr . Circles: calculated line (see text).

The line broadening is the greatest for $H // \langle 111 \rangle$ and the least for $H // \langle 001 \rangle$ (10 G). Charge compensation in the vicinity of the impurity cannot fully account for the broadening, since the same results are observed on the divalent isoelectronic $(3d^3) \text{V}^{2+}$ ion [3].

1.2 TETRAGONAL SITES (A AND A' LINES). — The superhyperfine structure, shown in figure 4, of the lines denoted A arises from a fluorine octahedron which is distorted along the cubic axes. This result excludes charge compensation by an O^{2-} ion replacing a nearest-neighbour F^- ion [4] and proves the lack

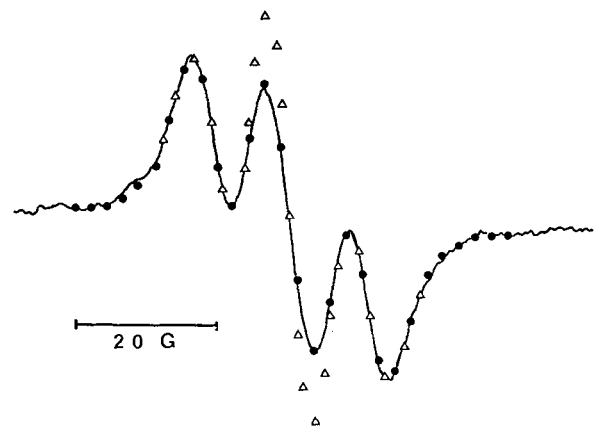


FIG. 4. — Tetragonal site (A): shf structure of the EPR line for the $|\frac{3}{2}\rangle \leftrightarrow |\frac{1}{2}\rangle$ transition. H is along a $\langle 001 \rangle$ axis. Full line: experimental curve. Circle: calculated line. Fit occurs with two unequivalent fluorine nuclei (F_1, F_2) along the distortion axis (see Table I). Triangle: calculated line assuming two equivalent (F_1, F_2) fluorine nuclei.

of a center of symmetry at the site. Charge compensation by O^{2-} impurity along $\langle 001 \rangle$ cannot explain the distortion, since doping the melt with Cr_2O_3 , during crystals growth, does not enhance neither the relative intensity of A lines nor the intensity of the A' lines.

We suggest that the A lines are due to pairing of a Cr^{3+} ion with a Zn^{2+} vacancy at a nn site. Similar value of the crystal field parameter ($D = 587 \text{ G}$) have been obtained for Cr^{3+} -nn Mg^{2+} vacancy pairs in MgO [5] ($D = 887 \text{ G}$).

The A' lines appear only in heavily doped crystals. The crystal field parameter $D_{A'}$ is twice D_A (Table I).

The replacement of Zn^{2+} ion by a K^+ ion in a nn site seems to be excluded because of a large ionic radius for K^+ . The pairing of a Cr^{3+} ion and of a Na^+ impurity ion is another possibility. Careful examination has shown that several, less intense, lines exist in the vicinity of the A' lines and more investigations have to be carried out to identify this defect. A similar defect has been observed in $\text{KZnF}_3 : \text{Fe}^{3+}$ (Table I).

1.3 TRIGONAL SITE (B LINE). — Angular dependence, with H rotating in the $(0\bar{1}0)$ plane, of the lines denoted B is shown in figure 5. The associated defect

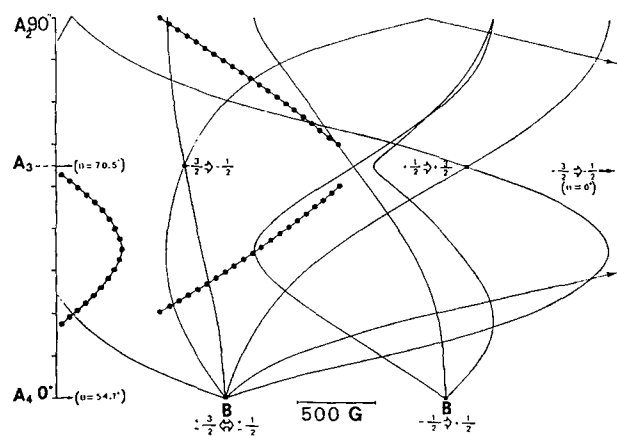


FIG. 5. — Trigonal site : Angular dependence with H rotating in a $(0\bar{1}1)$ plane of the lines denoted B . Full line : $|\Delta M_s| = 1$ transition. Circle : forbidden transition.

has obviously the trigonal symmetry. Forbidden lines ($\Delta M_s \neq 1$) arise from the large value of the crystal field parameter ($D = 1640$ G).

The simplest model, to account for the properties of this defect, is the pairing of a Cr^{3+} ions with a K^+ vacancy at a nearest neighbour site. A similar defect has been already observed in $\text{KZnF}_3 : \text{Fe}^{3+}$ crystals [4].

2. Optical absorption measurements on irradiated crystals. — The experiments have been carried out on a (001) plate ($10 \times 6 \times 4$ mm) obtained by means of a Bridgman-Stockbarger technique.

2.1 X-rays irradiation at room temperature, develops two bands at 230 and at 390 nm. The first band is expected to be due to a F-center.

Between 10 K and 300 K, the variation with temperature of the half-width for the 390 nm band, fits the law :

$$W(T) = W(0) \coth \left(\frac{\hbar\omega}{2kT} \right)^{1/2}$$

The value of the frequency of the dominant interacting phonon mode is $\omega = 3.4 \times 10^{13} \text{ s}^{-1}$, the extrapolated value of the band width at 0 K is

0.40 eV, the Huang-Rhys factor is $S = 64$. Bleaching the crystal at LNT with 313 nm light polarized along the cubic axis does not induce any dichroism, while bleaching with light polarized along the binary axis induces a dichroism in the optical absorption, as shown in figure 6b. The result is consistent with a

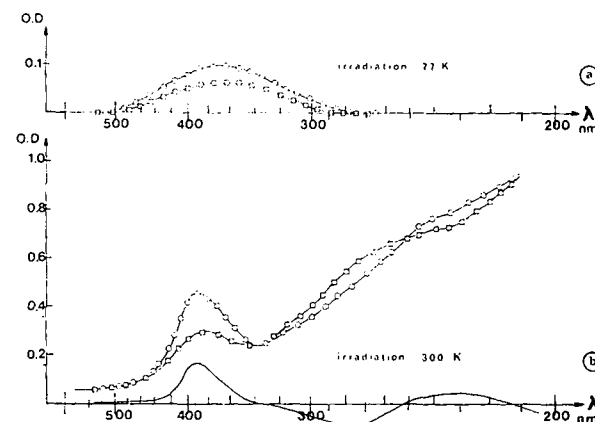


FIG. 6a. — Irradiation and bleach at LNT, with 365 nm light. Circle : $\text{OD}_{\langle 100 \rangle} - \text{OD}_{\langle 010 \rangle}$, bleach along $\langle 010 \rangle$. Square : $\text{OD}_{\langle 110 \rangle} - \text{OD}_{\langle \bar{1}\bar{1}0 \rangle}$, bleach along $\langle 1\bar{1}0 \rangle$.

FIG. 6b. — Irradiation at room temperature bleach at LNT with $\langle 110 \rangle$ polarized 313 nm light. Circle : OD at LNT $\langle 110 \rangle$ polarized light. Square : OD at LNT $\langle 1\bar{1}0 \rangle$ polarized light.

defect oriented along the ternary axis. More over two other bands more clearly appear at 270 nm and at 230 nm. The observed bands may be assigned, assuming a C_{3v} symmetry of the defect, to the following transitions :

$$\begin{aligned} 395 \text{ nm} &\rightarrow E \rightarrow A \\ 270 \text{ nm} &\rightarrow E \rightarrow E \\ 230 \text{ nm} &\rightarrow E \rightarrow A \end{aligned}$$

The optical properties of this center are similar to those of a R center observed by Riley and Sibley [7] in KMgF_3 . In our case more investigation have to be done to propose a definitive model for this center.

2.2 At LNT, X-rays irradiation develops the F band and a broad composite band on the long wavelength side of the F band. Bleaching at LNT, with either (010) or (110) polarized light 365 nm light or the $(\bar{1}\bar{1}0)$ axis, induces dichroism in the 360 nm region, as shown in figure 6a. The associated band is due to a defect, oriented along the binary axes. Moreover warming the crystal to 120 K, makes the band to disappear.

The observed properties of this defect are consistent with a F_2^- center, which has been already observed in KMgF_3 [7].

References

- [1] KRAVITZ, L. C. and PIPER, W. W., *Phys. Rev.* **146** (1966) 322.
[2] LEBLE, Thèse 3^e cycle juin 1973.
[3] DAVIES, J. J., SMITH, S. R. P., OWEN, J. and HANN, B. F., *J. Phys. C* **5** (1972) 245.
[4] KREBS, J. J. and JECK, R. K., *Phys. Rev.* **B 5** (1972) 3499.
[5] WERTZ, J. E. and AUZINS, P., *Phys. Rev.* **106** (1957) 484.
[6] JECK, R. K. and KREBS, J. J., *Phys. Rev.* **B 5** (1972) 1677.
[7] RILEY, C. R. and SIBLEY, W. A., *Phys. Rev.* **B 1** (1970) 2789.